COMPUTATIONAL STUDY ON THE INFLUENCE OF COANDA JET ON AIRFOILS: TWO-DIMENSIONAL CASE

H. Djojodihardjo* and M.F. Abdul Hamid**
Department of Aerospace Engineering, Universiti Putra Malaysia, Malaysia
* Professor and Corresponding author; email:harijono@djojodihardjo.com; ** Tutor and Graduate Student

Abstract

The influence of Coanda effect for lift generation and enhancement, following renewed interest elsewhere, is investigated using CFD simulation. To that end, attention is focussed on two-dimensional configuration and Coanda-Jet located at the trailing edge, to reveal the key elements that could exhibit the desired performance criteria for lift enhancement and drag reduction, or a combination of both. Parametric studies are carried out to obtain some optimum configuration, by varying pertinent airfoil geometrical and Coanda-Jet parameters. Particular attention is also given to turbulence modelling, by meticulous choice of appropriate turbulent models and scaling, commensurate with the grid generation, CFD code utilized and computational effectiveness. The present two-dimensional Coanda-Jet studies are carried out with wind turbine and micro-air-vehicle design in view.

1. Introduction

The progress of Computational Fluid Dynamics (CFD) has spurred renewed interest in further investigation on Coanda effect and its use to enhance lift [1- 7, 9, 14-17]. Tangential jets that take advantage of Coanda effect to closely follow the contour of the body can lead to increased circulation in the case of airfoils, or drag reduction (or drag increase if desired) in the case of bluff bodies such as an aircraft fuselage. Optimizing an airfoil's performance characteristics for the appropriate Reynolds number and thickness provides additional performance enhancement in the range of 3% to 5% [21]. For this purpose, the concepts of circulation control through trailing edge blowing, or Coanda-jets, could be explored. The state of affairs is depicted in Fig.1, where the Circulation Control on the Wing Upper Surface is shown on a a STOL Aircraft [2, 28]. The principlenof Coanda-effect jet tangential blowing over trailing edge surface for Lift Enhancementis exhibitrd inn Fig. 1 (b) [3]. Since CFD has progressed significantly and allowed numerical approaches that are based on the laws of conservation of mass, momentum, and energy in greater details, numerical simulation using CFD could be utilized to reveal and capture the physics of fluid flow behaviour near the flow boundaries, and could be useful in investigating related state of affairs of Coanda-jet configured aerodynamic surfaces.

To minimize the energy losses due to roughness effects and to develop special-purpose airfoils for Horizontal Axis Wind Turbine (HAWT's), the National Renewable Energy Laboratory (NREL), formerly the Solar Energy Research Institute (SERI), and Airfoils Inc. began a joint airfoil development effort in 1984 to produce a new series of airfoils, among others S809 airfoil [22-23], which are considered more appropriate for HAWT applications. These airfoils have been claimed to exhibit less sensitivity to roughness effects and better lift-to-drag ratios, and are recommended for retrofit blades and most new wind turbine designs [24]. In order to obtain results that can be well assessed, especially with reference to extensive research carried out as

described in [18-24], S809 airfoil [22-23] is considered in the present work.

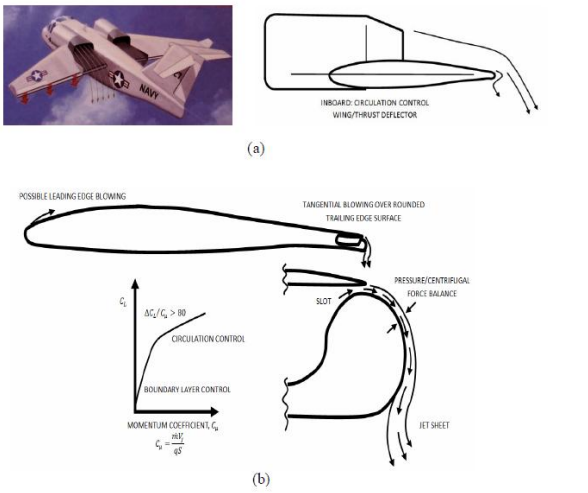

Fig. 1 (a) Circulation Control Wing/ Upper Surface Blowing STOL Aircraft Configuration, from [2, 28]; (b) Coanda-effect jet tangential blowing over trailing edge surface for Lift Enhancement, from [3]

To reveal the key elements that could lead to the desired lift enhancement and drag reduction, or a combination of both., without losing generalities and furthering previous studies [25-27], the present work critically reviews and looks into two-dimensional S809 airfoil in subsonic flow with Coanda-Jet located at its trailing edge. For benchmarking, in addition to a clean S809 airfoil, the GTRI Dual Radius CCW airfoil, which have already been investigated thoroughly, is also utilized. Parametric studies are useful in obtaining general ideas on optimum configuration, and are carried out by varying pertinent airfoil geometrical and Coanda-jet parameters. The numerical investigations carried out have in view applications for energy extraction system, such as wind turbine, and flight system, such as micro-air vehicles.

2. CFD Computational Modeling and Considerations of Turbulence Model

The computational studies capitalize on two-dimensional incompressible Reynolds-averaged Navier-Stokes (RANS) equation for the analysis using commercial CFD code COMSOL® [29]. The corresponding governing equation is given by the well known equation (steady state and ignoring body forces):

$$\rho\bar{u}_j\frac{\partial\bar{u}_i}{\partial x_j}=\frac{\partial}{\partial x_j}\left[-p\delta_{ij}+\mu\left(\frac{\partial\bar{u}_i}{\partial x_j}+\frac{\partial\bar{u}_j}{\partial x_i}\right)-\rho\overline{u_i'u_j'}\right] \quad (1)$$

In order to insure good modelling of the problem and obtain plausible computational results, several key issues are critically reviewed and validated using parallel analysis based on first principles as well as using other baseline numerical computation. An analysis based on physical considerations is also carried out with reference to its application in wind-turbine blade configuration.

The choice of grid fineness in CFD turbulence modeling and obtaining the correct simulation of particular flow field is very essential. The turbulent viscosity models based on Reynolds Averaged Navier-Stokes (RANS) equations (1) are commonly employed in CFD codes due to their relative affordability [40]. An appropriate model out of a host of available turbulence models developed to date has to be chosen. Judging from its generic clarity and user-friendliness, the $k-\varepsilon$ turbulence model is adopted, without disregarding other models that may be suitable for the purpose of the present work.

The $k-\varepsilon$ turbulence model was first proposed by Harlow and Nakayama [30, 31], in 1968, and further developed by Jones and Launder [32-35]. Continuing extensive research is carried out to understand the nature of turbulence, such as elaborated in [36-39]); various turbulence models seem to be satisfactory for only certain classes of cases. Since the choice of turbulence model and associated physical phenomena addresed are relevant in modeling and computer simulation of the flow situation near the airfoil surface, a closer look at turbulence models utilized by the CFD code chosen will be made. Although the practical implementation of turbulence model, especially for the near-wall treatment, has been some somewhat a mystery, the numerical implementation of turbulence models has a decisive influence on the quality of simulation results. In particular, a positivity-preserving

discretization of the troublesome convective terms is an important prerequisite for the robustness of the numerical algorithm [40]. The $k-\varepsilon$ model introduces two additional transport equations and two dependent variables: the turbulent kinetic energy, k, and the dissipation rate of turbulence energy, ε. Turbulent viscosity is modeled by using the Komolgorov-Prandtl formula

$$\mu_\tau = \rho C_\mu \frac{k^2}{\varepsilon} \qquad (2)$$

where C_μ is a model constant. The turbulent viscosity μ_τ in expression (2) was first introduced by Boussinesq [41] to draw analogy to the viscosity in laminar flow and for convenience of further analysis.

The dimensionless distance in the boundary layer, sub-layer scaled, representing the viscous sub-layer length scale, plays significant role in capturing relevant physical turbulence phenomena near the airfoil surface commensurate with the grids utilized in the numerical computation. In this regards, the flow field in the vicinity of the airfoil surface is usually characterized by the law of the wall, which attempts to identify intricate relationships between various turbulence scaling in various sublayers. For example, the wall functions approach (wall functions were applied at the first node from the wall) utilized by $k-\varepsilon$ turbulence model uses empirical laws to model the near-wall region [40] to circumvent the inability of the $k-\varepsilon$ model to predict a logarithmic velocity profile near a wall. The law of the wall is characterized by a dimensionless distance from the wall as defined by

$$y^+ = \frac{u_\tau y}{\upsilon} \qquad (3)$$

Subject to local Reynolds number considerations, the wall y+ is often used in CFD to choose the mesh fineness requirements in the numerical computation of a particular flow.

Various studies [38, 42] have indicated that integrating of the $k-\varepsilon$ type models through the near-wall region and applying the no-slip condition yields unsatisfactory results. Therefore, taking into account the need for effective choice of grid mesh compatible with the turbulence model adopted using the commercial CFD code, a parametric study is carried out on two airfoils where either experimental data or computational results are available. The objective is to validate the computational procedure, turbulence model and grid size chosen and establish their plausibility for further application in the present work. The idea is to place the first computational nodes outside the viscous sublayer, and make suitable assumptions about how the near-wall velocity profile behaves, in order to obtain the wall shear stress. Hence, the wall functions can be used to provide near-wall boundary conditions for the momentum and turbulence transport equations, rather than conditions at the wall itself, so that the viscous sublayer does not have to be resolved and the need for a very fine mesh is circumvented. The wall functions in COMSOL™ are chosen such that the computational domain is assumed to start at a distance y from the wall (see Fig. 2).

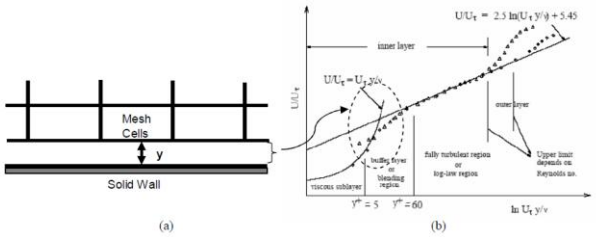

Fig. 2: For wall functions, the computational domain starts a distance y from the wall. (a) Depicted from COMSOL CFD Module User's Guide; (b) Depicted from FLUENT User's Guide

By applying the wall function at the nodes of the first meshing layer of the computational grid at a distance y from the wall (airfoil) surface, practically the meshing-layer of width y is removed from the computational domain, thus reducing the total number of grids involved, and hence reducing the computational time. Kuzmin [30] has introduced a wall function that is able to control the y+ value such that the y distance will not fall into the viscous sublayer, which could jeopardize the wall function assumption made. The smallest distance of y+ that can be

defined, following Grotjans and Menter [43], corresponds to the point where the logarithmic layer meets the viscous sublayer.

The distance y is automatically computed iteratively by solving $y^+ = \frac{1}{k}\log y^+ + \beta = \frac{1}{0.41}\log y^+ + 5.2$, so that $y^+ = \frac{u_\tau y}{\upsilon} = \rho u_\tau \left(\frac{y}{\mu}\right)$, where $u_\tau = \rho C_\mu \frac{k^2}{\varepsilon}$ (which has been further derived by Kuzmin et al [30] to be equivalent to $u_\tau = C_\mu^{\frac{1}{4}}\sqrt{k}$) is the friction velocity, and is equal to 11.06 (Kuzmin [38]). This corresponds to the distance from the wall where the logarithmic layer meets the viscous sublayer. Hence, the value of y, as represented by the choice of the computational grid size, can never becomes smaller than half of the height of the boundary mesh cell [38], as illustrated in Fig. 2(a). This means that y^+ can become larger than 11.06 if the mesh is relatively coarse.

Therefore, care is exercised in the choice of grids in the vicinity of the airfoil, to obtain a certain acceptable error tolerance (which may also be attributable to numerical error and uncertainties). The plausibility of the numerical results will be judged by comparison to other established results in the literature (numerical or experimental) for specific cases.

3. Computational Grid Generation and Validation

3.1. Computational Grid

In the present work, the grids were constructed following free mesh parameter grid generation using an algebraic grid generator and varied from extremely coarse up to extremely fine grids. However, for the S809 airfoil case, near the surface of the airfoil, boundary-layer based meshing is carried out throughout. Grid sensitivity study on the lift force per unit span for clean airfoil at zero angle of attack is plotted in Fig. 3.

Fig. 3 shows that the slope of the line starting from fine meshing grid size becomes stable after fine grid is generated. Therefore, the present analysis can be assumed to have an acceptable grid size with the choice of grid size in the range of *fine* up to *extra fine* grid size since within this range the lift as well as the drag forces does not change appreciably. The range of free mesh parameters (ranging from *extra fine* to *fine* meshing grid size) are defined in Table 1.

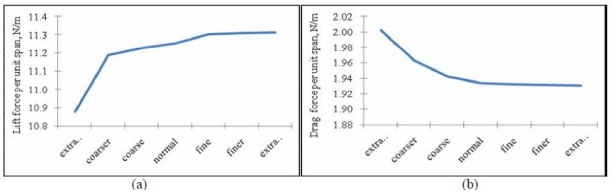

Fig. 3: Grid sensitivity study for clean S809 airfoil at zero degree angle of attack; (a) Lift force per unit span; (b) Drag force per unit span.

Table 1
The range of free mesh parameters

Parameter	Range
Maximum element size	0.156 – 0.42
Minimum element size	0.018 – 0.12
Maximum element growth rate	1.08 - 1.13
Resolution of curvature	0.25 - 0.3
Resolution of narrow regions	1

Table 2
Computational grid meshing-layer properties

Parameter	Range
Number of mesh layers in the boundary layers	8
Boundary layer mesh stretching factor	1.2
Thickness of first mesh layer	0.00005 – 0.0002
Thickness adjustment factor	1

In order to control the y+ value (set at 11.06, on the airfoil surface), the maximum element size was set at 0.005, while at the TE rounding-off surface the maximum element size was set at 0.001. At the Coanda jet outlet, the surface is divided into a minimum of 10 grid meshes.. To obtain acceptable computational results using COMSOL™ code, appropriate boundary layer mesh properties should be carefully chosen and the thin boundary layers along the no-slip boundaries should be resolved into mesh layers commensurate with the grid fineness. A boundary layer mesh is a quadrilateral mesh (2D

fluid flow) with dense element distribution in the normal direction along specific boundaries to resolve the thin boundary layers along the no-slip boundaries. The boundary layer properties chosen are defined in Table 2.

Along with the requirement of the y+ value to capture the salient turbulent flow field sublayers, a range of values of the grid dimension could be chosen to represent the thickness of the first meshing sublayers. In the present example the grid dimension were chosen to be between 0.00005m – 0.0002m, commensurate with the curvature on the airfoil surface. Having chosen the thickness of the elements of the first meshing layer adjacent to the airfoil surface, the following consecutive layers were stretched with a stretching factor of 1.2, for eight consecutive layers. Using COMSOL™ , another option is made available to allow the thickness adjustment of the first meshing layer, by choosing the thickness adjustment factor; for the present study, the thickness adjustment factor of one was chosen.

The grid generator is sufficiently general so that one can easily vary the jet slot location and size. Grid spacing and clustering can have significant effects on wind turbine load and performance predictions [36]. The outer boundary is placed far away from the blade surface, at least at six chord lengths (6C) from the airfoil surface, to avoid significant influence from outer boundary into the interior domain and to allow the disturbances to leave the domain [16]. The computational domain and the grid in the vicinity of the airfoil surface and Coanda-jet slot are exhibited in Fig. 4.

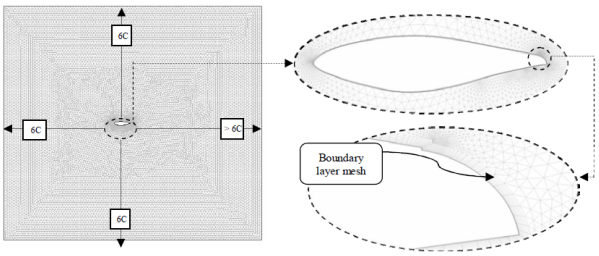

Fig. 4: Computational Grid around a Typical Airfoil, shown here for S809 Airfoil

3.2. Initial and Boundary Conditions

In general, the initial conditions are set to be equal to the properties of the free-stream flow condition. The flow properties everywhere inside the flow field are assumed to be uniform and set to the free-stream values. The following initial values are used:

$$u = u_\infty, \qquad v = v_\infty \qquad \rho = \rho_\infty \qquad (4)$$
$$p = p_\infty \qquad T = T_\infty$$

The outer boundary is placed far away from the blade surface, at a minimum of 6 chords (6C). Non-reflecting boundary conditions are applied at the outer boundaries of the computational domain. The jet is set to be tangential to the blade surface at the Coanda-jet nozzle location. The jet velocity profile is specified to be uniform at the jet exit. On the airfoil surface, except at the jet exit, no-slip boundary conditions are applied. To gain benefits, the jet velocity should be designed to be larger than the potential flow velocity at the vicinity of the outer edge of the boundary layer. In addition, the thickness of the Coanda jet is designed to be less than the local boundary layer thickness.

3.3. Baseline Validation

Prior to its utilization, various baseline cases have been tried out, with favorable results. As a case in point, for benchmarking purposes the code has been applied to calculate the lift-slope characteristics of S809 airfoil (clean configuration, without Coanda) and GTRI CCW Dual Radius airfoil (with Coanda), and compared to the results obtained by Somers [44] and Englar et al [3] respectively. The results as shown in Figs. 5 and 6 demonstrated its plausibility for the present investigation.

Computational results exhibited in Fig. 5 served to validate the computational procedure associated with the use of COMSOL™ code in the numerical simulation and as a baseline in furthering the computational study of Coanda jet in the present study. Fig. 5 compares the present computational simulation using $k-\varepsilon$ turbulence model and Kuzmin's [38] wall

function (the associated y+ value is 11.06) with the experimental data of Somers [43]. The numerical results above simulated similar experimental conditions of Somers for clean S809 airfoil (with wall boundary conditions and without Coanda jet). It also shows that the lift and drag coefficient at zero angle of attack are in close agreement with the experimental data.

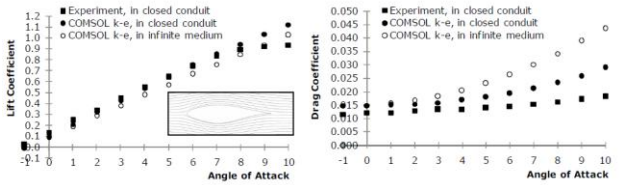

Fig. 5: Comparison for validation of S809 airfoil of CFD computational results using COMSOL® k-e turbulence model and experimental values from Somers (NREL [33]) at Re = 1E6; (a) Lift coefficient; (b) Drag coefficient.

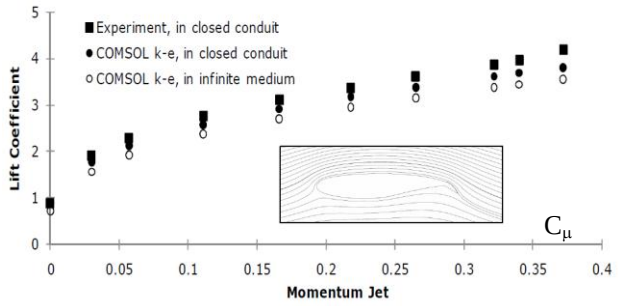

Fig. 6: Comparison of lift-curve slope for GTRI Dual Radius CCW airfoil with LE blowing on CFD computation

Similar numerical simulation was carried out for GTRI Dual Radius CCW airfoil with leading edge blowing and compared to the experimental data (in Fig. 6) from Jones and Englar [5]with the same boundary conditions and jet configuration using $k-\varepsilon$ turbulence model and Kuzmin's wall function. Of significant interest are the grid size, the wall function and y+ value utilized for numerical simulation. The associated y value for the cells adjacent to the airfoil surface was designed to be no more than 0.0002m in order to satisfy the y+ value requirements, which were chosen to be 11.06. The results exhibited in Fig. 6 for this case is also encouraging due to the close agreement between the present computation and the experimental data.

The results exhibited in both examples above serve to indicate, that the computational procedure and choice of turbulence model seem to be satisfactory for the present computational study, and could lend support to further use of the approach in the numerical parametric study.

All computations in the present study were performed on a laptop computer with a 2.10 GHz Intel Core Duo processor, 4 GB of RAM, and 32-bit Operating System. Typical computation time for the computation of the flow characteristics around a two dimensional airfoil is in the order of 4 hours with around 300,000 degrees of freedom by using stationary segregated solver in $k-\varepsilon$ turbulent model analysis. With such computational environment, which in consequence limits the computational grids, the present work will seek and adopt appropriate CFD numerical procedures. Simplified theoretical analysis is carried out prior to the modeling and numerical computation, while further theoretical analysis will be carried out in evaluating the computational results.

4. Results and Discussions

4.1. Design considerations for Coanda-configured Airfoil

For the purpose of assessing the influence and the effectiveness of the Coanda enhanced lift on wind-turbine blade, a generic two-dimensional study is carried out. The problem at issue is how the Coanda-jet can be introduced at the trailing edge of the airfoil, bearing in mind that such design may recover any losses due to the possible inception of flow separation there. In addition, for effective Coanda-jet performance, a curvature should be introduced. Furthermore, the thickness of the Coanda jet as introduced on the airfoil surface could have a very critical effect on the intended lift enhancement function. For best effect, the lower surface near the trailing edge should be flat, as suggested by Tongchitpakdee [18-19]. The design of the Coanda-configured trailing edge

should also consider the off-design conditions. With all these considerations, a configuration suggested is exhibited in Fig. 7.

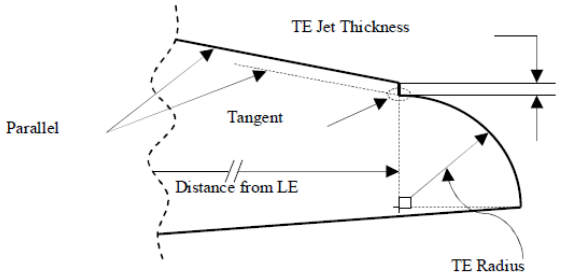

Fig. 7: Trailing edge construction of the Coanda configured airfoil (the jet flow is tangential to the rounded circular sector).

4.2. Computational results for S809 airfoil

Next, we would like to investigate the influence of specifically designed airfoil geometry for wind turbine application, and for this purpose a typical S809, in clean and Coanda-jet equipped configurations. S809 airfoil represents one of a new series of airfoils which are specifically designed for HAWT applications [18]. For the present study, the numerical simulation was carried out at two free-stream velocities. These are 5.77m/s (corresponding to Re = 3.95 x 10^5) and 14.6 m/sec (corresponding to Re = 1 x 10^6), which represent low and high free-stream cases, respectively, while the chord-length is maintained at c = 1m, and density at ρ = 1.225 kg/m^3. The baseline for assessing the advantages of Coanda-jet from parametric study on S809 airfoil is the computational result for the clean airfoil. The computational result for this baseline case has been validated by comparison of the computational value for the same S809 airfoil to the experimental results based on wind-tunnel test. It should be noted, that the flow field boundaries are different than those utilized for the parametric study.

The two-dimensional numerical simulation study for the S809 airfoil is carried out in logical and progressive steps. First, the numerical computation is performed on the clean S809 airfoil, then on the Coanda-jet configured S809 airfoil without the jet (i.e. after appropriate modification due to TE rounding-off and back-step geometry), and then finally on Coanda-jet configured S809 airfoil in its operational configuration.

To address three dimensional wind-turbine configurations, particularly for the optimum design of a Horizontal Axis Wind-Turbine (HAWT), logical adaptation should be made, taking into account the fact that different airfoil profiles may be employed at various radial sections. Certain assumptions have to be made in order to project two-dimensional simulation results to the three-dimensional case, which may be necessary to evaluate the equivalent Betz limit.

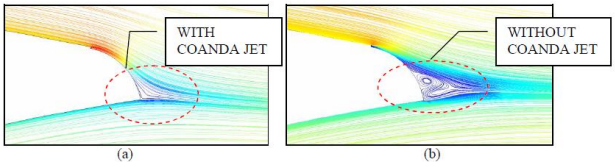

Fig. 8: Flow Fields of S809 Airfoil; (a) with, and (b) without - Coanda-jet.

The flow field in the vicinity of the trailing edge for both configurations is shown in Figs. 8a and 8b. Careful inspection of these figures may lead to the identification of the geometry of the flow that could contribute to increased lift, in similar fashion as that contributed by flap, jet-flap or Gurney flap. Fig. 8b typifies the flow field around Coanda configured S809 airfoil without Coanda-jet (only with its back-step configuration), for further reference.

The trailing edge radius plays an important role in the Coanda configured design airfoil, since it may positively or negatively influence the downstream flow behavior. Thongcitpakdee [18-19] had claimed that the lower surface at the TE of the applied Coanda jet should be flat in order to minimize the drag when the jet is turned off. Also, as reported earlier by Abramson and Rogers [44-45] in the late 1980's, in spite of ability to generate more lift, the technique has not in general been applied to production aircrafts. Many of the roadblocks

have been associated with the engine bleed requirements and cruise penalties associated with blown blunt trailing edges. In addition, there is a tradeoff between the use of a larger radius Coanda-configured airfoil for maximum lift and a smaller radius one for minimum cruise drag. In contrast to the needs of trailing edge rounding-off radius, performance degradation associated with it always stands as an issue due to the drag penalty when the jet is in the off mode. To overcome such draw-back, the TE radius should be specificallly and carefully designed. For that purpose, simulations at several TE radius (from 10mm to 50mm) have been performed, at a fixed Coanda-jet momentum coefficient C_μ ($C_\mu = 0.003$, considered just enough to fit with the wind turbine application), and at a constant free-stream velocity of $V_\infty = 14.6$ m/sec (Re= 1 x 10^6), to investigate the effect of TE radius on the aerodynamic characteristics of Coanda configured airfoils. Results exhibited in Fig. 9 show that a higher L/D can be achieved with a smaller TE radius (30 mm), and that the L/D is decreasing as the TE radius is increased from 30 mm to 50 mm. The effect of TE radius on the lift augmention does not seem to be significant, as exhibited by the dashed line in Fig. 9. However, when the TE radius is increased beyond certain value (in Fig. 9, >> 35 mm), the TE rounding-off seems to be ineffective, even detrimental.

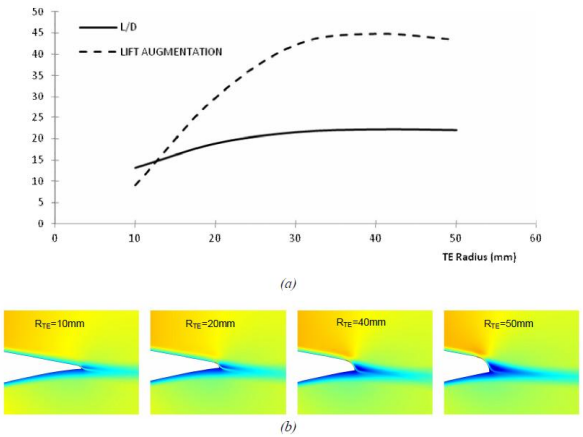

Fig. 9: (a) The effect of TE radius on L/D with Coanda jet; (b) Velocity flow field for different TE radius (Re = 1 x 10^6, $C_\mu = 0.005$, t_{jet} = 1 mm)

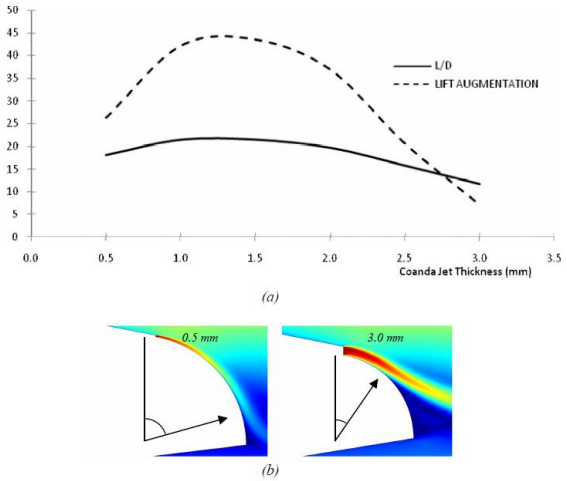

Fig. 10: (a) The effect of jet thickness on the L/D and lift augmentation; (b) Flow separation with different Coanda jet thickness (Re = 1 x 10^6, R = 10 mm $C_\mu = 0.005$,)

Variation of the Coanda jet thickness from 0.5 mm to 3.0 mm at a fixed C_μ ($C_\mu = 0.005$), and at a constant free-stream velocity of $V_\infty = 14.6$ m/sec (Re= 1 x 10^6) is performed to investigate the effect of Coanda jet thickness (also called jet-slot-thickness) on the aerodynamic characteristics of Coanda configured airfoils. From Fig. 10, it is found that a higher L/D can be achieved with a smaller Coanda jet thickness (1.0-1.5 mm), and that the L/D is decreased rapidly as the Coanda jet thickness is increased from 1.0 mm to 3.0 mm. A similar behavior is observed for the lift augmention as exhibited by the dashed line in Fig. 10. However, generating a smaller jet requires higher pressure than a larger one at the same momentum coefficient. Since higher lift with as low mass flow rate as possible is preferred, a thin jet is more beneficial than a thick jet [9]. From aerodynamic design perspective, within the range of agreeable power to generate Coanda-jet, a smaller Coanda jet thickness is preferred, although further careful trade-off study should be made.

The performance of Coanda configured airfoils is dependent on the jet momentum conditions, which are important driving parameters. Fig. 11 shows numerical simulation

for a free-stream velocity of 5.77 m/sec. At very low jet momentum coefficient $C_\mu << 0.005$, the jet velocity is too low to generate a sufficiently strong Coanda effects that eliminates separation and vortex shedding.

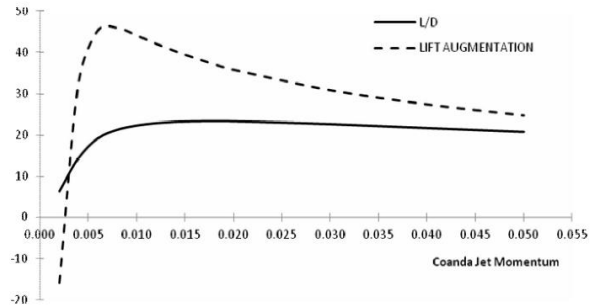

Fig. 11: The effect of jet momentum on the L/D and lift augmentation (Re = 3.95 x 10^5, R_{TE} = 50 mm, t_{jet} = 1 mm)

The lift to drag ratio L/D increases significantly with the increase of the jet momentum coefficient (C_μ) until the jet momentum coefficient reaches $C_\mu > 0.01$. After this value, the effect is otherwise. Under fixed free-stream velocity and fixed Coanda jet thickness, the total mass flow rate increases linearly with the increase of the jet momentum. Also the jet velocity ($V_{Coanda\text{-}jet}$) has to be increased with the mass flow rate to keep a constant C_μ. The dotted line shown in Fig. 12 shows that the maximum lift augmention is slightly above 60.

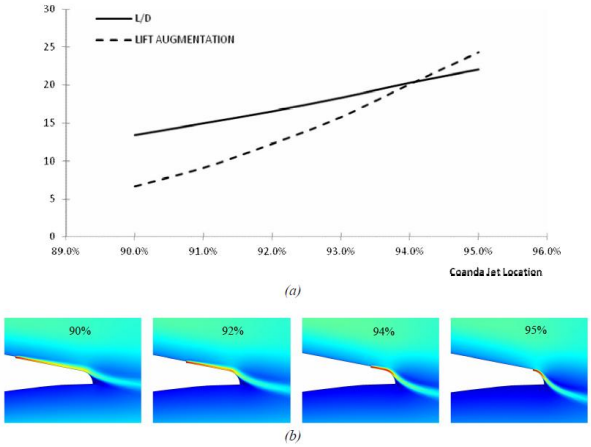

Fig. 12: (a) The effect of Coanda jet location on the L/D and lift augmentation; (b) Velocity flow field for different Coanda jet location (Re = 1 x 10^6, R_{TE} = 10 mm, t_{jet} = 1 mm, $C_\mu = 0.010$)

4.3. Performance Parameter:

It should be noted that for the purposes of the present work, a uniform jet velocity profile has been adopted; this could be readily modified for more realistic modeling or design requirements. Numerical results indicate that there exists an optimum Coanda-jet configuration, which has been the subject of parametric study as exhibited in Figs. 9 – 12 for S809 airfoil.

A significant performance design parameter which has been utilized to characterize Coanda-jet application by many investigators [8-9, 18-19], is specified by the momentum coefficient of the jet, C_μ. It represents the contribution of the Coanda-jet momentum to Wind-Turbine Input Power, or to the ideal maximum Wind-Turbine Power, if the Betz limit is considered. For two-dimensional modeling, an equivalent jet momentum coefficient C_μ^* can be defined as:

$$C_\mu^* \equiv \frac{\dot{m} V_{Coanda-jet}}{\frac{1}{2}\rho V_\infty^2 A_{ref}} = \frac{\rho_{Coanda-jet} V_{Coanda-jet} t_{Coanda-jet} t_{Coanda-jet}}{\frac{1}{2}\rho V_\infty^2 c_{airfoil}} \quad (5)$$

This expression shows that for a given constant C_μ, changing the thickness of the Coanda-jet will affect C_μ favorably.

To justify the results of the present study, and to give us a physical explanation of the effect of Coanda-jet, one may attempt to carry out simple calculation using first principle and Kutta-Joukowski law for potential flow, and compare the Lift of the Coanda-jet configured airfoil with the clean one obtained using COMSOL® CFD code.

$$L_{Coanda-jet\ Airfoil} = L_{clean\ Airfoil} + \rho V_\infty \left(V_{Coanda-jet} h_{Coanda-jet} \right) \quad (7)$$

where $h_{Coanda-jet}$ is the moment arm of the Coanda-jet with respect to the airfoil aerodynamic center.

One then may arrive at a very good conclusion on the contribution of the Coanda-jet to the lift (surprisingly, using COMSOL™ CFD results for the lift ($L_{Coanda-jet\ Airfoil}$) values, the accuracy obtained by using equation (3) was in the order of 1.39%). However, care should be exercised to insure valid modeling for comparison.

For the three-dimensional configuration, there is a physical relationship between the Wind-Turbine shaft torque (which is a direct measure of the shaft power extracted) with C_μ, and in the actual three-dimensional case, the wind-turbine rotor yaw angle [18-19]. From the numerical results gained thus far, it can be surmised that circulation control, which in this particular case obtained by utilizing Trailing-edge Coanda-jet, can considerably increases the torque generated through the L/D increase gained.

The maximum theoretical power that can be extracted from the free stream (ambient air) is given by the Betz limit:

$$P_{Betz} = \frac{8}{27}\rho A_{Wind-turbine\ rotor} V_\infty^{\ 2} \quad (6)$$

(where V_∞ is the free-stream wind speed). With the use of Coanda-jet, assuming the jet energy can be drawn from the inner part of the free-stream in the vicinity of the wind-turbine rotor hub, the Coanda-jet additional power output corresponding to the jet momentum coefficient should contribute to the increase of shaft power output given by the theoretical Betz limit. Tongchitpakdee studies [19] also indicated such results. It should be noted that the ambient air free-stream wind speed V_∞ for the Wind-Turbine is different from the V_∞ implied in the present two-dimensional parametric study, which is the resultant of the ambient-air wind speed and the rotational speed of the particular section of the rotor blade.

Using simple calculation from first principle, the power required for introducing Coanda-jet in a Wind-Turbine (three-dimensional) can be estimated, although the extent of such implementation depends on engineering ingenuity. However, it can safely be surmised that the Coanda-jet can be introduced by extracting free stream energy from the unproductive part of the air-flow.

5. Conclusion

CFD numerical experiments have been carried out to elaborate work reported earlier [26-28], with the objective to verify the favorable effects of Coanda-configured airfoil for enhanced aerodynamic performance and obtain some guidelines for the critical features of Coanda-jet configured airfoil. Care has been exercised in the choice of turbulence model and other relevant parameters commensurate with the grid fineness desired, in particular since the number of grid utilized is relatively small in view of the desk-top computer utilized capabilities. Comparison of the numerical computation results for some baseline cases with experimental data under similar conditions lends support to the present computational parametric study.

Two-dimensional parametric studies have shown the effectiveness of Coanda-jet in producing enhanced lift, which consequently will contribute to increased torque for wind turbine application, and increased axial thrust for propeller application. Guided by earlier results and using physical judgments, the Coanda-jet configured airfoil studied has been tailored to arrive at favorable aerodynamic performance. Parametric studies have been carried out to this end.

Rounding-off of the trailing edge for introducing Coanda-jet seems to be more convenient and effective in gaining L/D increase for Wind Turbine specifically designed airfoil, here exemplified by S809. Such result may be due to the relatively large trailing edge angle of the Wind Turbine Specifically designed airfoil, and may lead to better aerodynamic performance of such airfoil compared to the reference airfoil used as the baseline.

The results thus far obtained are computed for two-dimensional airfoil configuration, and their effects in modifying aerodynamic performance in general agree with those obtained for three dimensional results of Tongchitpakdee [15-16]. Hence the two-

dimensional numerical study can be used to direct further utilization of the CFD computational procedure to the three-dimensional Wind-Turbine blade studies and design optimization.

Numerical results presented have been confined to zero angle-of-attack case, which has been considered to be very strategic in exhibiting the merit of Coanda-jet as lift enhancer. The numerical studies could be extended to increasing angle of attack to obtain more comprehensive information, for which the choice of turbulence model will be more crucial.

Acknowledgements

The authors would like to thank Universiti Putra Malaysia (UPM) for granting Research University Grant Scheme (RUGS) No. 05-02-10-0928RU; CC-91933, under which the present research is carried out. The corresponding author would also like to thank Universitas Al-Azhar Indonesia for the opportunity to carry out the present research at Universiti Putra Malaysia.

6. Nomenclature

CFD	Computational Fluid Dynamic
CCW	Circulation Control Wing
R	Trailing edge radius (mm)
C	Airfoil chord length (m)
C_μ	Coanda Jet Momentum Coefficient
C_μ*	2-D equivalent of C_μ
L	Lift force (N)
D	Drag force (N)
H	Coanda jet thickness (mm)
L/D	Lift over drag ratio
R/C	Trailing edge radius over airfoil chord length ratio
H/C	Coanda jet thickness over airfoil chord length ratio
TE	Trailing Edge
STOL	Short Takeoff Landing
y^+	Dimensionless wall distance for a wall-bounded flow
u_τ	Friction velocity
y	Distance to the nearest wall
v	Kinematic viscosity
τ_w	Wall shear stress
ρ	Density
μ_τ	Turbulent Viscosity, as defined by Equation (2)
HAWT	Horizontal Axis Wind Turbine
M	Mach number
C_μ	Turbulent Model Constant, as defined by Equation (2)
C_μ	Momentum coefficient
$\frac{\Delta C_L}{C_L}$	Lift augmentation
MW	Megawatt
MWh	Megawatt hour

7. References

[1] Lan, C.E., Campbell, J.F., "Theoretical Aerodynamics of Upper-Surface Blowing Jet-Wing Interaction", NASA TN D-7936, November 1975.

[2] Harris, M.J., "Investigation of the Circulation Control Wing/Upper Surface Blowing High-Lift System on a Low Aspect Ratio Semispan Model", Report DTNSRDC/ASED-81/10, David Taylor Naval Ship R&D Center , Aviation and Surface Effects Department, Bethesda, Maryland 20084, May 1981.

[3] Englar, R.J., Smith M.J., Kelley, S.M., Rover, R.C., "Application of Circulation Control to Advanced Subsonic Transport Aircraft, Part I: Airfoil Development", Journal of Aircraft, vol. 31, no. 5, pp. 1160-1168, 1994.

[4] Englar, R.J., Smith M.J., Kelley, S.M., Rover, R.C., "Application of Circulation Control to Advanced Subsonic Transport Aircraft, Part II: Transport Application", Journal of Aircraft, vol. 31, no. 5, pp. 1169-1177, 1994.

[5] Jones, G. S., Englar, R. J., "Advances in Pneumatic-Controlled High-Lift Systems Through Pulsed Blowing", AIAA 2003-3411 21st Applied Aerodynamics Conference 23-26 June 2003 Orlando, Florida.

[6] Zhulev, Y.G., Inshakov, S.I., "On the Possibility of Enhancing the Efficiency of Tangential Blowing of a Slit Jet From an Airfoil Surface", Fluid Dynamics, vol. 31, no. 4, Plenum Publishing Corporation, 1996, Translated from Izvestiya Rossiiskoi Akademii Nauk, Mekhanika Zhidkosti i Gaza, no. 4, pp. 182-186, July-August, 1996. Original article submitted February 14, 1995.

[7] Gad-el-Hak, M., "Modern Developments in Flow Control", in Applied Mechanics Reviews, vol. 49, pp. 365–379, 1996.

[8] Englar, R.J., "Advanced Aerodynamic Devices to Improve the Performance, Economics, Handling and Safety of Heavy Vehicles", SAE Technical Paper Series 2001-01-2072, 2001.

[9] Liu, Y., Sankar, L.N., Englar, R.J., Ahuja, K., "Numerical Simulations of the Steady and

Unsteady Aerodynamic Characteristics of a Circulation Control Wing", AIAA 2001-0704, 39th AIAA Aerospace Sciences Meeting, Reno, NV, 2001.

[10] Liu, Y., "Numerical Simulations of the Aerodynamic Characteristics of Circulation Control Wing Sections", PhD Dissertation, Georgia Institute of Technology, May 2003.

[11] Wu, J., Sankar, L.N., Kondor, S., "Numerical Modelling of Coanda Jet Controlled Nacelle Configuration", Paper AIAA-2004-0228, 42nd AIAA Aerospace Science Meeting and Exhibit, Reno, Nevada, 5- 8 Jan 2004.

[12] Mamou, M., Khalid, M., "Steady and Unsteady Flow Simulation of a Combined Jet Flap and Coanda Jet Effects on a 2D Airfoil Aerodynamic Performance", Revue des Energies Renouvelables CER'07 Oujda, pp. 55-60, 2007.

[13] Shojaefard, M.H., Noorpoor, A.R., Avanesians, A., Ghaffarpour, M., "Numerical Investigation of Flow Control by Suction and Injection on a Subsonic Airfoil", American Journal of Applied Sciences 2, vol. 10, pp. 1474-1480, 2005.

[14] Sinha, S.K., "Optimizing Wing Lift to Drag Ratio Enhancement with Flexible-Wall Turbulence Control", AIAA-2007-101APA21, 2007.

[15] Radespiel, R., Pfingsten, K.C., Jensch, C., "Flow Analysis of Augmented High-Lift Systems", TU Braunschweig, Institut für Strömungsmechanik, Bienroder Weg 3, D-38108 Braunschweig, Germany, Hermann Schlichting- 100 Years Memorial Volume, NNFM 102, pp. 168-189, Springerlink.com, © Springer-Verlag Berlin Heidelberg, 2009.

[16] Hokpunna, A., Manhart, M., "A Large-Eddy Simulation of Vortex Cell flow with Incoming Turbulent Boundary Layer", World Academy of Science, Engineering and Technology 32, 2007.

[17] Kral, L.D., "Active Flow Control Technology", ASME Fluids Engineering Technical Brief, 2000.

[18] Tongchitpakdee, C., "Computational Studies of the Effects of Active and Passive Circulation Enhancement Concepts on Wind Turbine Performance", PhD Dissertation, Georgia Institute of Technology, August 2007.

[19] Tongchitpakdee, C., Benjanirat, S., Sankar, L.N., "Numerical Studies of the Effects of Active and Passive Circulation Enhancement Concepts on Wind Turbine Performance", Journal of Solar Energy Engineering, Transactions of the ASME, vol. 128, pp. 432-444, 2006.

[20] Xu, G., Sankar, L. N., "Computational Study of Horizontal Axis Wind Turbines", UASME Journal of Solar Energy Engineering, vol. 122, no. 1, pp. 35-39, 2000

[21] Xu, G., "Computational Studies of Horizontal Axis Wind Turbines", PhD. Dissertation, School of Aerospace Engineering, Georgia Institute of Technology, Atlanta, GA, 2001.

[22] Tangler, J.L. et al., "SERI Advanced Wind Turbine Blades", International Solar Energy Society Conference, Denver, Colorado, 1991.

[23] Tangler, J.L., Somers, D.M., "NREL Airfoil Families for HAWTs", American Wind Energy Association, NREL/TP-442-7109, UC Category: 1211, DE95000267, 1995.

[24] Duque, E.P.N., Johnson, W., van Dam, C.P., Cortes, R., Yee, K., "Numerical Predictions of Wind Turbine Power and Aerodynamic Loads for the NREL Phase II Combined Experiment Rotor", AIAA-2000-0038, 38th AIAA Aerospace Sciences Meeting, Reno, NV, 2000.

[25] Abdul-Hamid, M. F., Djojodihardjo, H., Suzuki, S., Mustapha, F., "Numerical Assessment of Coanda Effect as Airfoil Lift Enhancer in Wind-Turbine Configuration", paper RCMEAE-131, Proceedings, Regional Conference on Mechanical and Aerospace Technology, Bali, February 9-10, 2010.

[26] Djojodihardjo, H., Abdul Hamid, M.F., "Review and Numerical Analysis of Coanda Effect Circulation Control for Wind-Turbine Application Considerations", Conference on Aerospace and Mechanical Engineering, World Engineering Congress 2010, 2nd – 5th August 2010, Kuching, Sarawak, Malaysia.

[27] Djojodihardjo, H., Abdul-Hamid, M.F., Basri, S.N., Romli, FF.I. and Abdul-Majid, D.L.AS., Numerical Simulation And Analysis Of Coanda Effect Circulation Control For Wind-Turbine Application Considerations, IIUM Journal, to appear, 2011.

[28] Day, T., "The Coanda Effect And Lift", Copyright 2008. terry@vortex-dynamics.com. au;http://www. newfluidtechnology.com. au/THE_COANDA _EFFECT_AND_LIFT.pdf.

[29] COMSOL™ 4.2. CFD Module User's Guide.

[30] Harlow, F.H. and Nakayama, P.,"Turbulence Transport Equations"-Physics of Fluids, Vol.10, No.11, 1967

[31] Harlow, F.H. and Nakayama, P.,"Transport of turbulence energy decay rate", Los Alamos Science Laboratory, University of California Report LA-3854, 1968.

[32] Launder, B.E., Morse, A., Rodi, W. and Spalding, D.B., The prediction of free shear flows - A comparison of the performance of six turbulence models, Proceedings of NASA Conference on Free Shear Flows, Langley (1972) (Also Imperia1 College Mechanical Engineering Department Report TM/TN/A/19).

[33] Launder, B.E. and Sharma, B.I., "Application of the Energy-Dissipation Model of Turbulence to the Calculation of Flow Near a Spinning Disc", Letters in Heat and Mass Transfer, Vol. 1, No. 2, pp. 131-138, 1974.

[34] W.P. Jones and B.E. Launder, Predictions of low-Reynolds-number phenomena with a Z-equation

model of turbulence, Intern. J. Heat & Mass Transfer 16 (1973) p. 1119.
[35] W.P. Jones, B.E. Launder, "The Prediction of Laminarization with a Two-Equation Model of Turbulence", International Journal of Heat and Mass Transfer, vol. 15, 1972, pp. 301-314, 1972.
[36] Rumsey, C.L., Spalart, P.R., "Turbulence Model Behavior in Low Reynolds Number Regions of Aerodynamic Flow fields", 38th AIAA Fluid Dynamics Conference and Exhibit, Seattle, WA, June 23-26, 2008.
[37] Menter, F.R., "Advances in Turbulence Modelling of Unsteady Flows", ANSYS, Germany, © 2009 ANSYS, Inc, 2009; also Menter Shear Stress Transport Model, http://turbmodels.larc.nasa.gov/sst.html
[38] Kuzmin, D., Mierka, O., Turek, S., "On the Implementation of the k-e Turbulence Model in Incompressible Flow Solvers Based on a Finite Element Discretization", International Journal of Computing Science and Mathematics, vol. 1, no. 2–4, pp. 193–206, 2007.
[39] Wilcox, D.C., "Turbulence Modeling for CFD", 3rd Edition, DCW Industries, 2006.
[40] Benjanirat, S., "Computational Studies of Horizontal Axis Wind Turbines in High Wind Speed Condition using Advanced Turbulence Models", PhD. Thesis, Georgia Institute of Technology, December 2006.
[41] Boussinesq, J., "Essai sur la théorie des eaux courantes", Mémoires présentés par divers savants à l'Académie des Sciences 23 (1): 1-680, 1877.
[42] S.M. Salim, S.C. Cheah, "Wall y+ Strategy for Dealing with Wall-bounded Turbulent Flows", Proceedings of the International Multi-Conference of Engineers and Computer Scientists 2009 Vol. II, IMECS 2009, Hong Kong, March 18 - 20, 2009..
[43] Grotjans, H. and Menter, F. (1998), Wall Functions for General Application CFD Codes, ECCOMAS 98, Proceedings of the 4th Computational Fluid Dynamics Conference, John Wiley & Sons, pp.1112-1117.
[44] Somers, D.M., "Design and Experimental Results for the S809 Airfoil," Airfoils, Inc., State College, PA, 1989.
[45] Abramson, J., Rogers, E.O., "High-speed Characteristics of Circulation Control Airfoils," AIAA-83-0265, January 1988.
[46] Rogers, E.O., "Development of Compressible Flow Similarity Concepts for Circulation Control Airfoils," AIAA-87-0153, January 1987.

Acknowledgement

The authors would like to thank Universiti Putra Malaysia (UPM) for granting Research University Grant Scheme (RUGS) No. 05-02-10-0928RU; CC-91933, under which the present research is carried out.

Copyright Statement